Conductivity and Dielectric Response in the Ion-Exchange Intercalated Mono- and Double-Layer Hydrates $Cd_{0.75}PS_3Na_{0.5}(H_2O)_y$, $y = 1, 2$

P. Jeevanandam and S. Vasudevan*

Department of Inorganic and Physical Chemistry, Indian Institute of Science, Bangalore, India

Received: September 10, 1997; In Final Form: November 24, 1997

Hydrated Na ions have been ion-exchange intercalated into the insulating layered cadmium thiophosphate to give $Cd_{0.75}PS_3Na_{0.5}(H_2O)_y$. Intercalation occurs with a dilation of the lattice which depends on the extent of hydration of the interlamellar Na ion; for $y = 1$ the lattice expansion is 2.8 Å, while for $y = 2$ it is 5.5 Å. The conductivity and dielectric response of $Cd_{0.75}PS_3Na_{0.5}(H_2O)_y$, $y = 1, 2$, have been investigated as a function of frequency and temperature. The electrical behavior of the two compounds is dramatically different. In the $y = 2$ compound Na ions are mobile and the material is conducting. The dielectric spectrum is featureless, but the electrical modulus, the reciprocal of the complex dielectric permittivity, exhibits a conductivity relaxation. In contrast, when $y = 1$, the compound is nonconducting, with the dielectric permittivity exhibiting a relaxation. The relaxation times and activation energy are comparable to that of the dielectric relaxation at acoustic frequencies in ice.

1. Introduction

The layered divalent metal thiophosphates, MPS_3 where M is Cd, Mn, or Fe, undergo an unusual ion-exchange intercalation reaction in which hydrated cations from an aqueous solution insert into the interlamellar space with an equivalent loss of the divalent ion from the layer, leaving immobile vacancies.[1,2] The metal thiophosphates may be viewed as being formed by the stacking of MPS_3 layers, which in turn have been built from edge-shared MS_6 and P_2S_6 polyhedra.[3] The van der Waals gap between the sheets is 3.2 Å (Figure 1). Intercalation occurs with a dilation of the lattice along the interlayer axis, the extent of which depends on the nature of the guest cation and the extent of its hydration. For cadmium thiophosphate the reaction may be written as

$$CdPS_3 + 2xNa^+ \rightarrow Cd_{1-x}PS_3Na_{2x}(H_2O)_y + xCd^{2+} \qquad x = 0.25, \quad y = 2$$

where the guest species, hydrated Na ions, reside in the interlamellar space and the reaction consequently proceeds with a lattice expansion, Δd, of 5.5 Å. The extent of hydration, the value of y, in these compounds is usually determined by thermogravimetry. We found that the thermal deintercalation of water from the as-prepared $Cd_{1-x}PS_3Na_{2x}(H_2O)_y$, $y = 2$, compound occurs in two steps, and we were able to identify the first step as the formation of a $Cd_{1-x}PS_3Na_{2x}(H_2O)_y$ phase with $y = 1$ and lattice expansion, Δd, of 2.8 Å. The conversion of the $y = 2$ "double-layer" to the $y = 1$ "monolayer" phase is completely reversible (Figure 1). These compounds, therefore, present a unique opportunity to investigate the conductivity and dielectric behavior for differing extents of hydration of the intercalated guest cation. In addition, the negatively charged $Cd_{0.75}PS_3$ layers in these compounds are electrically inert;[4] consequently the observed response can be attributed, entirely, to the intercalated hydrated Na ions.

The intercalated $Cd_{1-x}PS_3Na_{2x}(H_2O)_y$ bear resemblance to the mica-type silicate (MTS) clays, e.g., Na-montmorillonite. These are layered aluminosilicates, idealized composition $Al_4(Si_4O_{10})_2(OH)_4 \cdot xH_2O$, in which isomorphous substitution in the tetrahedral and octahedral sites by lower valent cations requires the inclusion of interlayer cations, which are usually hydrated, to maintain charge balance. Montmorillonite clays have been cited as examples of inorganic ion-exchange materials showing fast protonic conduction.[5] The conductivity of the clays is known to show a strong dependence on the extent of hydration of the interlayer cation, decreasing in magnitude with increasing loss of water.[6] In Na-vermiculite, there is evidence that the Na ions too are mobile and contribute to the conductivity. Here too, a decrease in mobilities with dehydration has been observed.[7,8] A similar dependence of conductivity on the extent of hydration of the Na ion may be anticipated for $Cd_{1-x}PS_3Na_{2x}(H_2O)_y$ ($y = 1, 2$) and has indeed been observed.

We have carried out a detailed investigation of the ac electrical response in $Cd_{1-x}PS_3Na_{2x}(H_2O)_y$ ($y = 1, 2$) as a function of frequency and temperature. The electrical behavior of the two compounds is dramatically different. In the $y = 2$, "double-layer" hydrate, the Na ions are mobile and the material is conducting. In contrast, the "monolayer" $y = 1$ hydrate is insulating, with the dielectric permittivity exhibiting a relaxation at acoustic frequencies.

2. Experimental Section

Cadmium thiophosphate, $CdPS_3$, was prepared from the elements following the procedure reported in ref 9. Cadmium metal powder, phosphorus, and sulfur in stoichiometric amounts were sealed in a quartz ampule at 10^{-5} Torr and heated at 650 °C for a period of two weeks. The formation of $CdPS_3$ was confirmed by powder X-ray diffraction; the pattern could be indexed in the $C2/m$ space group with lattice parameters $a = 6.313$ Å, $b = 10.787$ Å, $c = 6.906$ Å, and $\beta = 108.35°$, similar to that reported in the literature.[10]

$Cd_{1-x}PS_3Na_{2x}(H_2O)_y$ can be prepared by the direct ion-exchange intercalation reaction; however, a more facile route is by exchanging the K^+ ions in $Cd_{1-x}PS_3K_{2x}(H_2O)$ with Na

S1089-5647(97)02945-3 CCC: $15.00
Published on Web 03/31/1998

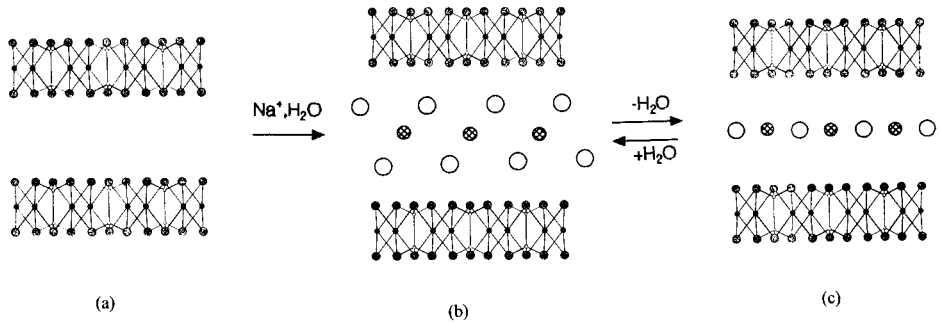

Figure 1. Schematic of the layered cadmium thiophosphates: (a) the parent $CdPS_3$, (b) the double-layer, $y = 2$, $Cd_{0.75}PS_3Na_{0.5}(H_2O)_y$, and (c) the monolayer, $y = 1$, $Cd_{0.75}PS_3Na_{0.5}(H_2O)_y$. Dotted circles = S; small open circles = P; solid circles = Cd; large open circles = H_2O; hatched circles = Na ion (cadmium ion vacancies are not shown).

ions. The potassium ion-exchanged intercalation compound was obtained by stirring $CdPS_3$ powder in an aqueous solution of KCl along with a complexing agent, EDTA. Complete ion-exchange intercalation was ascertained by the absence of $CdPS_3$ *00l* reflections and the appearance of new *00l* reflections with a lattice spacing, *d*, of 9.3 Å. $Cd_{1-x}PS_3Na_{2x}(H_2O)_y$ in turn was obtained by the following ion-exchange reaction.

$$Cd_{1-x}PS_3K_{2x}(H_2O)_z + 2xNa^+_{aq} \rightarrow Cd_{1-x}PS_3Na_{2x}(H_2O)_y + 2xK^+_{aq}$$

Ion-exchange of the K ions by Na ions causes the lattice spacing to increase from 9.3 Å to 12.1 Å.

Cadmium and sodium ion stoichiometries were established by atomic absorption spectrometry (AAS) after dissolving the compound in aqua regia. The value of *x* is 0.25. Phosphorus and sulfur stoichiometries were not estimated and assumed to be the same as that in $CdPS_3$. The value of *y*, the extent of hydration, was determined by thermogravimetric measurements in air using a Cahn 2000 microbalance. Powder X-ray diffraction was recorded on a Shimadzu XD-D1 diffractometer using Cu- Kα radiation. Room-temperature ^{23}Na NMR (resonance frequency 79.3 MHz) were recorded on a Bruker DSX-300 spectrometer.

Electrical measurements were made on pelletized samples using platinum electrodes. Sample temperature could be varied from 30 to 330 K with ±0.5 K accuracy using a closed cycle cryostat (CTI-cryogenics). The complex admittance, $Y^* = Y' + iY''$, was measured in the frequency range $10-10^5$ Hz using a dual-phase lock-in analyzer (PAR 5208).[11] The physical quantities of interest, the real and imaginary parts of the complex dielectric permittivity and the complex electrical modulus,[12] M^*, which is the reciprocal of the complex dielectric permittivity, ϵ^*, were derived from the complex admittance, Y^*. $\epsilon^* = Y^*/i\omega C_0$, where C_0 is the vacuum capacitance of the cell; $C_0 = \epsilon_0 A/d$. *A* is the area of the electrode, *d* is the thickness of the sample, and $\epsilon_0 = 8.854 \times 10^{-12}$ F/m. The conductance (σ_{DC}) was extracted from the complex admittance data.

In a typical experiment, a pellet of $Cd_{0.75}PS_3Na_{0.5}(H_2O)_2$ was placed in the cryostat and cooled, *without* evacuation, to 278 K. At this temperature the cryostat was evacuated for a short period (30 s), to avoid condensation on the sample and on the inner walls of the cryostat. The cryostat was then isolated and the sample cooled to 250 K. At this temperature the cryostat was reconnected to the vacuum system and cooled to the lowest temperature. The above procedure was necessary to avoid any decomposition of the "double-layer" $Cd_{0.75}PS_3Na_{0.5}(H_2O)_2$ to the insulating "monolayer".

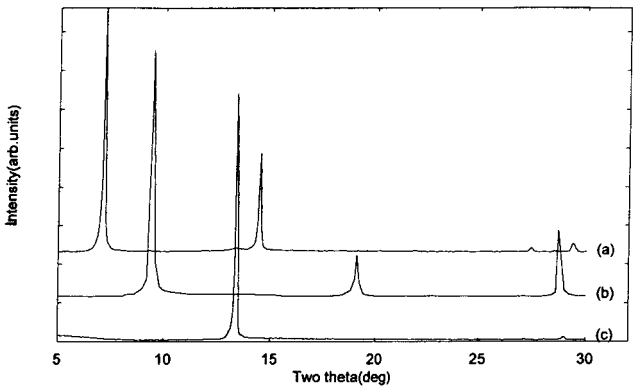

Figure 2. Powder XRD of (a) the double-layer $Cd_{0.75}PS_3Na_{0.5}(H_2O)_2$, (b) the monolayer $Cd_{0.75}PS_3Na_{0.5}(H_2O)$, and (c) $CdPS_3$.

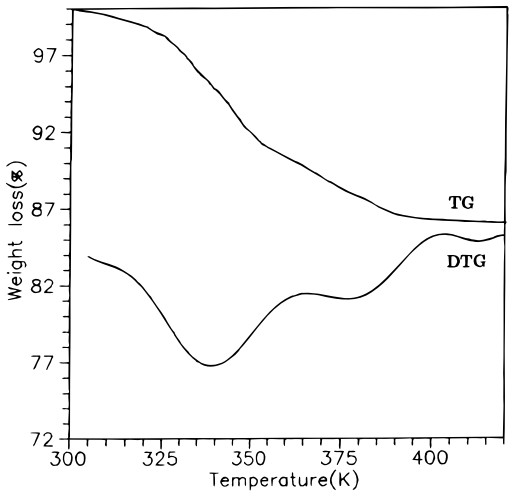

Figure 3. TG and differential thermogram (DTG) of $Cd_{0.75}PS_3Na_{0.5}(H_2O)_2$.

3. Results and Discussion

The X-ray diffraction pattern of $Cd_{1-x}PS_3Na_{2x}(H_2O)_y$ ($y = 2$) is shown in Figure 2. The pattern could be indexed in the same space group as that of $CdPS_3$, *C*2/*m*, with lattice parameters $a = 6.578$ Å, $b = 10.013$ Å, $c = 12.875$ Å, and $\beta = 108.85°$. A comparison with the parameters of $CdPS_3$ shows that the change corresponds to a lattice expansion, Δd, of 5.5 Å. As mentioned earlier, the extent of hydration, the value of *y*, was determined by thermogravimetry (TG). The TG of the as-prepared $Cd_{1-x}PS_3Na_{2x}(H_2O)_y$ showed a total weight loss of 18%, corresponding to a value of $y = 2$. It may be seen from Figure 3 that the thermal deintercalation of water occurs in two steps. This may be more clearly seen in the differential

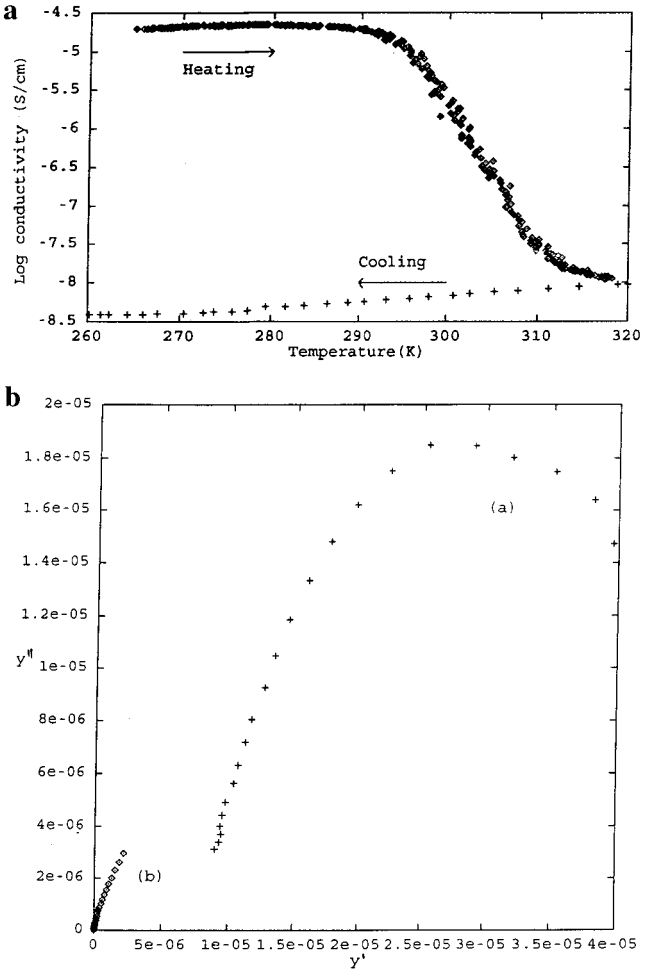

Figure 4. (a) Conductivity as a function of temperature for $Cd_{0.75}PS_3Na_{0.5}(H_2O)_2$ at 1 kHz. (b) Complex admittance plot at 250 K of (a) the double-layer $Cd_{0.75}PS_3Na_{0.5}(H_2O)_2$ and (b) the monolayer $Cd_{0.75}PS_3Na_{0.5}(H_2O)$.

thermogram. The first step occurs at 343 K with a weight loss of 9.2%, corresponding to the formation of $Cd_{1-x}PS_3Na_{2x}(H_2O)_y$ with $y = 1$. If the TG is stopped at this temperature and the sample cooled, the original weight is recovered. A similar weight loss, corresponding to the formation of a $y = 1$ phase, is observed when $Cd_{1-x}PS_3Na_{2x}(H_2O)_y$, $y = 2$, compounds are evacuated at 10^{-2} Torr at room temperature. On exposure to the atmosphere, the original weight corresponding to the $y = 2$ phase is recovered. The results imply that the conversion of the $y = 2$ to $y = 1$ phase is completely reversible. The X-ray diffraction pattern of the $y = 1$ phase recorded under vacuum is shown in Figure 2 (due to the preferred orientation of the crystallites, only the *00l* reflections were observed).

The lattice spacing d is 9.3 Å, corresponding to a lattice expansion Δd of 2.8 Å. Since the lattice expansion is close to the diameter of a water molecule, 2.8 Å, the $y = 1$ phase will be referred to as the monolayer hydrate and the $y = 2$ phase with $\Delta d = 5.5$ Å as the double-layer hydrate. This nomenclature is similar to that used in the mica-type silicate clays.[13] Complete dehydration of the $Cd_{1-x}PS_3Na_{2x}(H_2O)_y$ compounds leads to a partial collapse of the $Cd_{0.75}Na_{0.5}PS_3$ lattice. Consequently when TG runs are stopped at 405 K (Figure 3) and the samples cooled, the original weight is not recovered. In this respect the behavior is different from that of the clays. In many clays, e.g., vermiculite, the integrity of the phyllosilicate layers is preserved even on complete dehydration of the interlamellar cation.

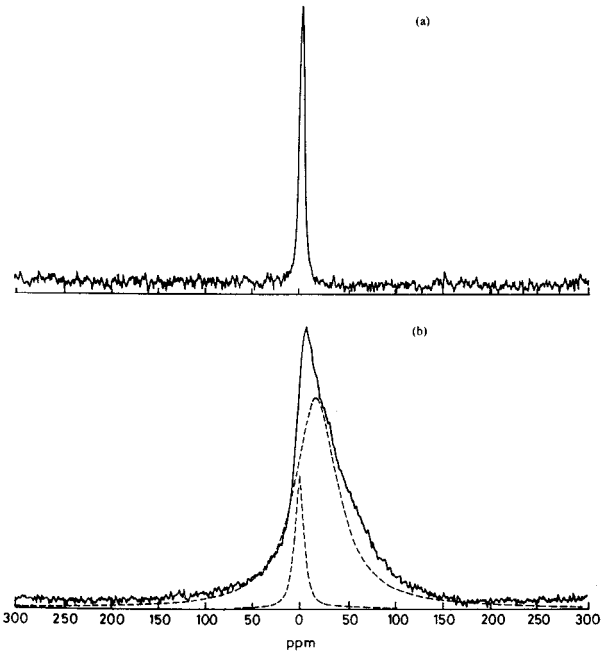

Figure 5. Room-temperature static ^{23}NMR spectra of (a) the double-layer $Cd_{0.75}PS_3Na_{0.5}(H_2O)_2$ and (b) the monolayer $Cd_{0.75}PS_3Na_{0.5}(H_2O)$. The deconvoluted spectra are shown in dashed lines.

The $Cd_{1-x}PS_3Na_{2x}(H_2O)_y$, $y = 1$, phase is rapidly converted to the $y = 2$ phase on exposure to air. Consequently for the electrical measurements the monolayer sample was prepared in situ within the cryostat by the decomposition of the double-layer $y = 2$ phase. The large difference in the conductivity between the double-layer and monolayer hydrates provided a convenient way of monitoring the progress of the decomposition. In a typical experiment, a pellet of $Cd_{0.75}PS_3Na_{0.5}(H_2O)_2$ was placed in the cryostat, evacuated at 10^{-2} Torr at 278 K, and then cooled to 250 K. The temperature was then raised linearly at 1°/min. During heating the total conductivity, $\sigma(\omega) = \omega\epsilon_0\epsilon''$, usually at 1 kHz or 100 Hz, was monitored. In Figure 4a, the total conductivity at 1 kHz of $Cd_{0.75}PS_3Na_{0.5}(H_2O)_2$ is shown as a function of temperature. The sample was under dynamic vacuum (10^{-2} Torr). The sharp drop in conductivity from 4.3×10^{-5} to 4.09×10^{-9} S/cm between 290 and 310 K signifies the formation of the "monolayer" $Cd_{0.75}PS_3Na_{0.5}(H_2O)$ sample. On subsequent cooling, under vacuum, the conductivity is not reversible but follows the cooling curve shown in Figure 4a and has a value of 3.98×10^{-9} S/cm at 250 K. As long as the vacuum is not broken, the sample may be heated and cooled any number of times, with the conductivity closely following the bottom curve in Figure 4a. If at room temperature, the "monolayer" compound is exposed to the atmosphere, the high conductivity associated with the "double-layer" is recovered.

The complex admittances of the monolayer, $y = 1$, and double-layer, $y = 2$, phases of $Cd_{1-x}PS_3Na_{2x}(H_2O)_y$ at 250 K have been plotted in Figure 4b. The intercept on the real axis of the complex admittance plot is the dc conductance (σ_{DC}).[14] It may be seen that there is a dramatic decrease in the conductance values from $\sigma_{DC} = 4.3 \times 10^{-5}$ S/cm for the $y = 2$ phase to $\sigma_{DC} = 4.09 \times 10^{-9}$ S/cm for the $y = 1$ phase.

To determine whether the interlamellar Na ions are mobile, the room-temperature static ^{23}Na NMR spectra of the $y = 2$ and $y = 1$ phases of $Cd_{0.75}PS_3Na_{0.5}(H_2O)_y$ were recorded. The ^{23}Na NMR of the $y = 2$ phase shows a single sharp Lorentzian (fwhm = 5.5 ppm) (Figure 5). The study of the monolayer $y = 1$ phase was more difficult because of partial rehydration to the $y = 2$ phase during transfer. Contamination by the $y = 2$

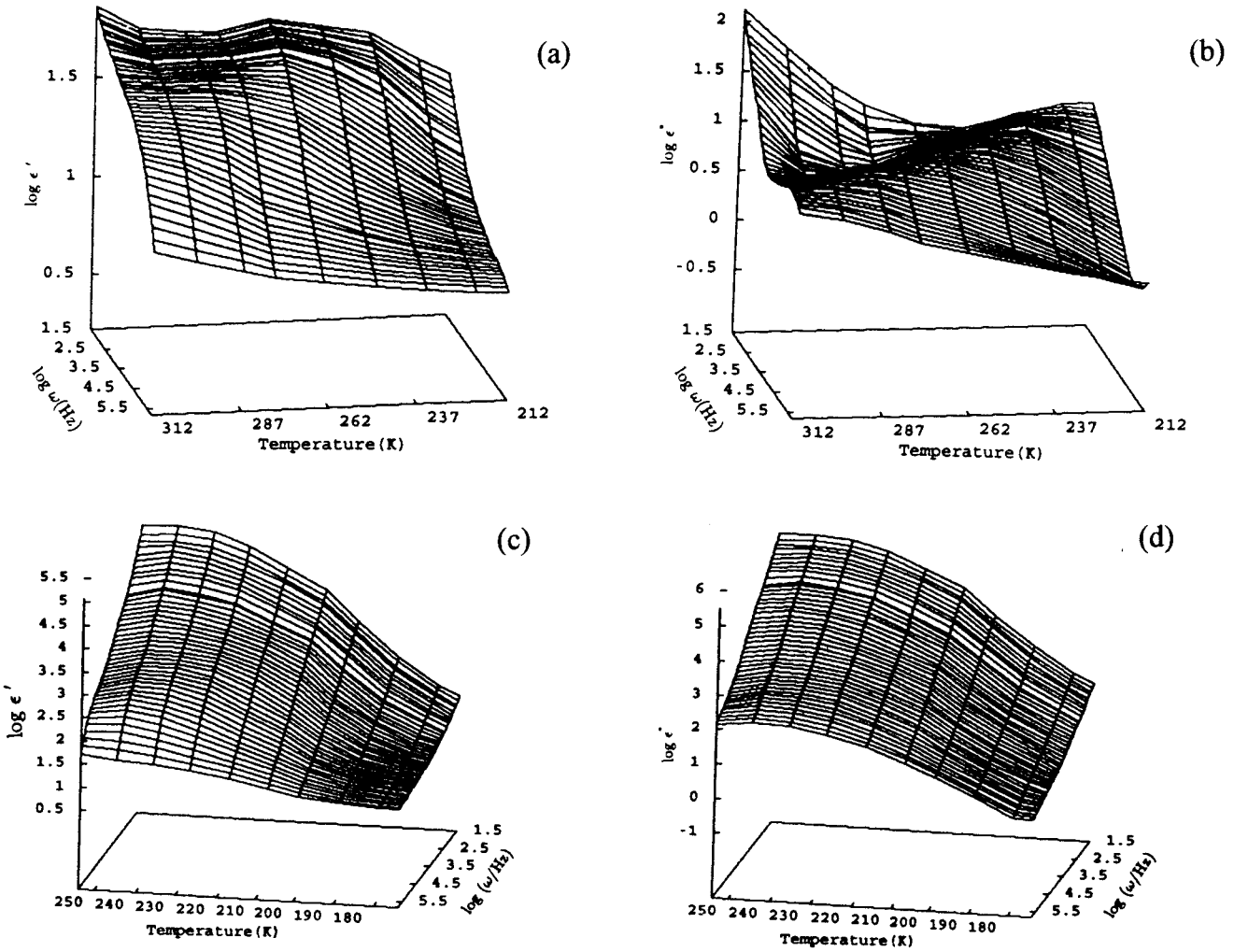

Figure 6. Real and imaginary components of the complex dielectric permittivity as a function of temperature for the monolayer, $Cd_{0.75}PS_3Na_{0.5}(H_2O)$ (a and b) and the double-layer $Cd_{0.75}PS_3Na_{0.5}(H_2O)_2$ (c and d).

phase may be evidenced from the skewed line shapes observed for the $y = 1$ phase (Figure 5). The spectra could, however, be consistently deconvoluted as two Lorentzians, one of which is centered at −18 ppm with a fwhm of 28 ppm and the other centered at 0 ppm with fwhm of 5.5 ppm. The latter component may be assigned to the $y = 2$ phase. For both compounds, the ^{23}Na NMR was recorded with a spectral window of ±300 ppm; it may be concluded that the $\pm 3/2 \Leftrightarrow \pm 1/2$ satellite cannot be observed. The narrow ^{23}Na NMR line width of the $y = 2$ phase may be interpreted as evidence for rapid Na ion motion so that chemical shift anisotropy and heteronuclear, ^{23}Na−^{1}H, dipolar interactions are averaged. The increase in line width on loss of water suggests a slowing of Na ion motion on formation of the $y = 1$ phase. These observations, including the downfield shift on dehydration, are similar to previous observations on the ^{23}Na NMR of Na-vermiculite at various levels of hydration.[15]

The temperature and frequency dependence of the real (ϵ') and imaginary(ϵ'') components of the complex dielectric permittivity of the $y = 1$ and $y = 2$ phases of $Cd_{1-x}PS_3Na_{2x}(H_2O)_y$ are shown in Figure 6a−d. The dielectric response in the insulating $y = 1$ monolayer phase is dominated by a loss feature, with the loss maxima moving to lower frequencies with decrease in temperature. Both ϵ' and ϵ'' of the $y = 1$ phase show a strong frequency dispersion at low frequencies (at high temperatures).

In contrast to the $y = 1$ phase, the ϵ'' spectra of the double-layer $y = 2$ phase show no maxima; instead, both the real and imaginary components show a simple dispersion in the present frequency−temperature window. The dispersion of ϵ'' is shown in Figure 7 in the form of a plot of the real part of the conductivity, $\sigma'(\omega)$, versus frequency, and the dispersion of ϵ' as a plot of $\log(\epsilon' - \epsilon_\infty)$ versus frequency. The real part of the frequency-dependent conductivity is related to the imaginary part of the permittivity, ϵ'', through the relation $\sigma'(\omega) = \epsilon''(\omega)\omega\epsilon_0$. In Figure 7a, the frequency dispersion of the conductivity for different temperatures has been plotted on a double logarithmic scale. The conductivity shows a sublinear frequency dependence and follows a simple power law dispersion,[16] $\sigma'(\omega) = \sigma_0 + A\omega^S$, where σ_0 is the dc conductivity, A is a temperature-dependent parameter, and S is a fractional exponent between 0 and 1 (the solid line in Figure 7a is the fit to this expression). This response is characteristic of hopping conductivity and has been "universally" observed in a number of ionic conductors.[14,16,17] The value of σ_0 obtained from the fits of Figure 7a are identical to the σ_{DC} values as obtained from the complex admittance. The fact that the complex conductivities are reasonably well described by $\sigma'(\omega) = \sigma_0 + A\omega^S$ over the entire frequency−temperature window indicates that the electrode polarization effects are not important in the present case. If present, electrode polarization would have shown up as a crossover to a stronger dispersion at low frequencies. Figure 7b shows the frequency dependence of the real part of the permittivity from which the high-frequency permittivity, ϵ_∞, has been subtracted, at different temperatures. The plots are linear with slopes less than unity. The ϵ' data of the $y = 2$

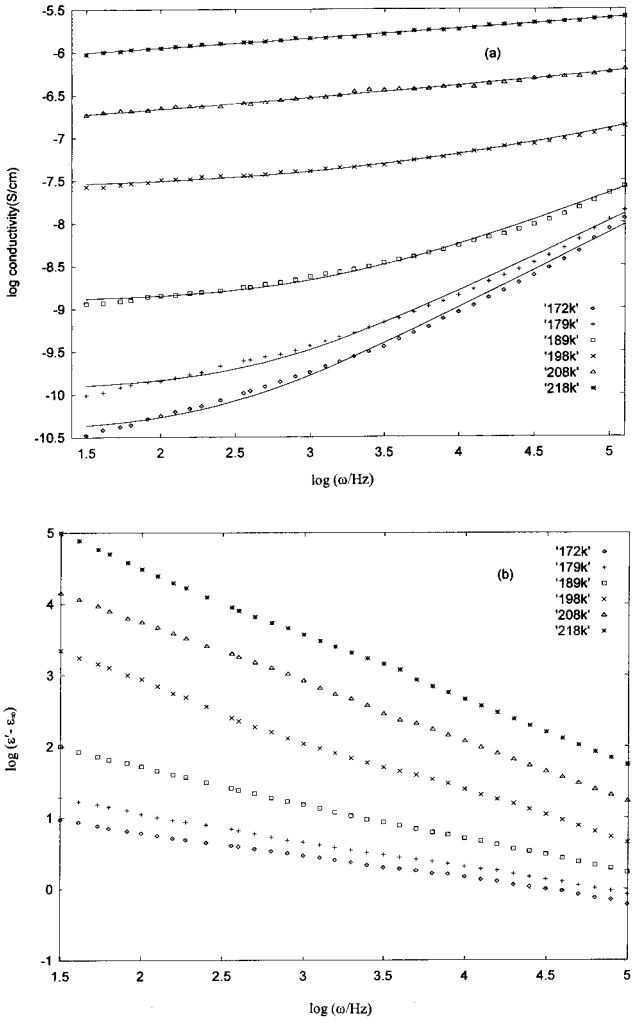

Figure 7. (a) Conductivity vs frequency for $Cd_{0.75}PS_3Na_{0.5}(H_2O)_2$ presented in a double-logarithmic scale at different temperatures. Solid lines are fits to the expression $\sigma'(\omega) = \sigma_0 + A\,\omega^S$. (b) ϵ' data, from which the high frequency value ϵ_∞ has been subtracted, vs frequency at different temperatures for $Cd_{0.75}PS_3Na_{0.5}(H_2O)_2$. Data are presented in a double-logarithmic scale.

phase provide further evidence that electrode polarization is not significant (it may be recalled that the limiting form for Maxwell−Wagner space charge polarization[18,19] is a power law dispersion $\epsilon' \sim \omega^{-2}$, $\epsilon'' \sim \omega^{-1}$).[14,20]

The electrical behavior of $Cd_{1-x}PS_3Na_{2x}(H_2O)_y$ clearly depends on the extent of hydration of the alkali cation. In the as-prepared $y = 2$ phase the Na ions are mobile and the material is conducting, whereas in the monolayer $y = 1$ phase the conductivity values are small and the dielectric response shows a loss feature in the complex permittivity. In the following sections the two compounds are discussed separately.

Dielectric Response of $Cd_{1-x}PS_3Na_{2x}(H_2O)_y$, $y = 1$. In the insulating monolayer $y = 1$ phase, the dielectric response is due to intercalated water molecules which hydrate the alkali ions; the contribution from the Na ions is unlikely to be significant since they are not mobile. As in the case of the mica-type silicate clays[13,21] and the monolayer $Cd_{1-x}PS_3A_{2x}(H_2O)$ [A = K,Cs],[22] the water molecules may be assumed to form a two-dimensional hydrogen-bonded network structure. The overall dielectric response has two contributions: (i) a polarization due to proton transfer on application of an electric field, creating OH^- and H_3O^+ at the end of a path, and (ii) polarization due to the reorientation of the permanent dipole moment

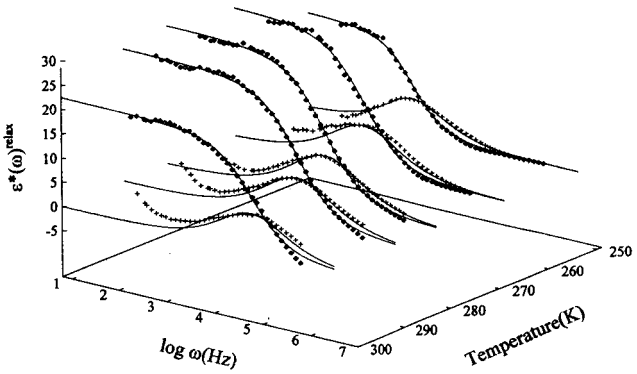

Figure 8. Real (◊) and imaginary (+) part of the dielectric relaxation, $\epsilon^*(\omega)^{relax}$, of the monolayer $Cd_{0.75}PS_3Na_{0.5}(H_2O)$. The solid line is the best fit to the HN equation (eq 1).

associated with the water molecules. In the subsequent analysis these are considered as independent processes and hence their contributions separable. The dielectric response due to proton hopping follows a power law dispersion, $\epsilon', \epsilon'' \sim a\omega^{-n}$ $(0 < n < 1)$.[14,23] The strong dispersion at low frequencies in Figure 6a,b may be attributed to this process.

To analyze the loss, it is necessary to separate out the contribution due to proton hopping. This may be evaluated by fitting the low-frequency data of Figure 6a,b to a power law dispersion.[22] Subtracting out the power law contribution from the experimental dielectric permittivity gives the contribution arising from relaxation processes, ϵ^{*relax}. This is shown in Figure 8.

The relaxation process was analyzed using the empirical Havriliak−Negami (HN) equation,[24,25]

$$\epsilon^*(\omega) = \epsilon_\infty + \frac{\epsilon_s - \epsilon_\infty}{(1 + (i\omega\tau)^{1-\alpha})^\beta} \qquad (1)$$

where $0 \le \alpha, \beta \le 1$ are the shape parameters. The real part of the HN equation,

$$\epsilon'(\omega) = \epsilon_\infty + (\epsilon_s - \epsilon_\infty)\frac{\cos\beta\varphi}{[1 + 2(\omega\tau_0)^{1-\alpha}\sin{}^1\!/_2\pi\alpha + (\omega\tau_0)^{2(1-\alpha)}]^{\beta/2}} \qquad (2)$$

where $\varphi = \text{arctg}[(\omega\tau_0)^{1-\alpha}\cos{}^1\!/_2\,\pi\alpha/(1 + (\omega\tau_0)^{1-\alpha}\sin{}^1\!/_2\,\pi\alpha)]$, was fitted to the experimental $\epsilon'(\omega)^{relax}$ data (Figure 8) by floating the HN parameters α, β, τ, and $(\epsilon_s - \epsilon_\infty)$. ϵ_s is the static permittivity. The HN fits to the experimental $\epsilon'(\omega)^{relax}$ data are shown as the solid line in Figure 8. The best-fit parameters are given in Table 1. The calculated $\epsilon''(\omega)^{relax}$ spectra using the best-fit HN parameters are also shown in Figure 8 along with the experimental data.

It is interesting to note that the best fits were always obtained for $\beta = 1$ (Table 1). A value of unity for β in eq 1 implies that the response obeys a Cole−Cole behavior characteristic of a symmetrical distribution of relaxation times with α characterizing the width of the distribution. The pure Debye process corresponds to $\alpha = 0$, $\beta = 1$ in eq 1. The mean relaxation time $\langle\tau\rangle$ associated with the Cole−Cole distribution shows an Arrhenius temperature variation with $E_a = 11.92$ kcal/mol.

Loss peaks due to the relaxation process have been observed in a number of hydrated samples at acoustic frequencies and have been attributed to the reorientation of the dipole moment associated with the H_2O molecules.[26,27] The values of τ for $Cd_{1-x}PS_3Na_{2x}(H_2O)_y$, $y = 1$, (Table 1) indicate that the

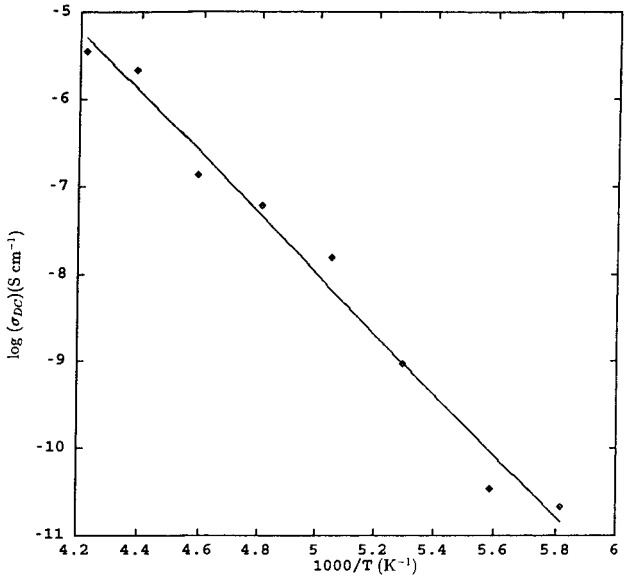

Figure 9. Temperature variation of the dc conductivity of the double-layer $Cd_{0.75}PS_3Na_{0.5}(H_2O)_2$. The solid line is the Arrhenius fit.

TABLE 1: Dielectric Relaxation Parameters for $Cd_{0.75}PS_3Na_{0.5}(H_2O)$

sample	temp (K)	τ (s)	α	β
$Cd_{0.75}PS_3Na_{0.5}(H_2O)$	249	8.45×10^{-4}	0.20	1.0
	264	3.15×10^{-4}	0.27	1.0
	278	8.21×10^{-5}	0.26	1.0
	287	3.85×10^{-5}	0.25	1.0
	300	1.68×10^{-5}	0.23	1.0
	312	7.62×10^{-6}	0.09	1.0
liquid water		9.30×10^{-12}	0.01	
ice I_h	250	3.0×10^{-6}	0.025	

reorientational motion of water molecules is on the same time scale as that in ice. The values of activation energies, too, are similar in magnitude to that of the dielectric relaxation at acoustic frequencies in ice, 13 kcal/mol.[28] This suggests that relaxation processes may be similar and may involve, for example, H-bond breaking followed by molecular rotation and subsequent bond recreation, similar to Bjerrum defect formation, which gives rise to the dielectric loss at acoustic frequencies in ice.[28,29] In ice the dielectric relaxation can quite accurately be described as a Debye process (or Cole−Cole with $\alpha = 0.02$). It is interesting to note that for $Cd_{1-x}PS_3Na_{2x}(H_2O)_y$, $y = 1$, the relaxation is well described by the symmetric Cole−Cole distribution, although the fitting of the data had been attempted for the more general Havriliak−Negami representation. The values of the α's in Table 1 indicate a variety of molecular environments for the intercalated water as compared to bulk ice.

Conductivity of $Cd_{1-x}PS_3Na_{2x}(H_2O)_y$, $y = 2$. The temperature variation of the dc conductivity of $Cd_{1-x}PS_3Na_{2x}(H_2O)_2$ (Figure 9) is Arrhenius, with an activation energy of 15.8 kcal/mol. This value is close to that observed in the bilayer mica-type silicates.[8]

The dispersion behavior of the conductivity in the frequency domain (Figure 7a) is more conveniently interpreted in terms of a conductivity relaxation time, τ_σ, using the electrical modulus, $M^* = 1/\epsilon^*$, representation.[12] Although originally conceived as a formalism to separate space-charge effects from the bulk conductivity, the M^* representation is now widely used to analyze ionic conductivities by associating a conductivity relaxation time, τ_σ, with the ionic process.[30,31]

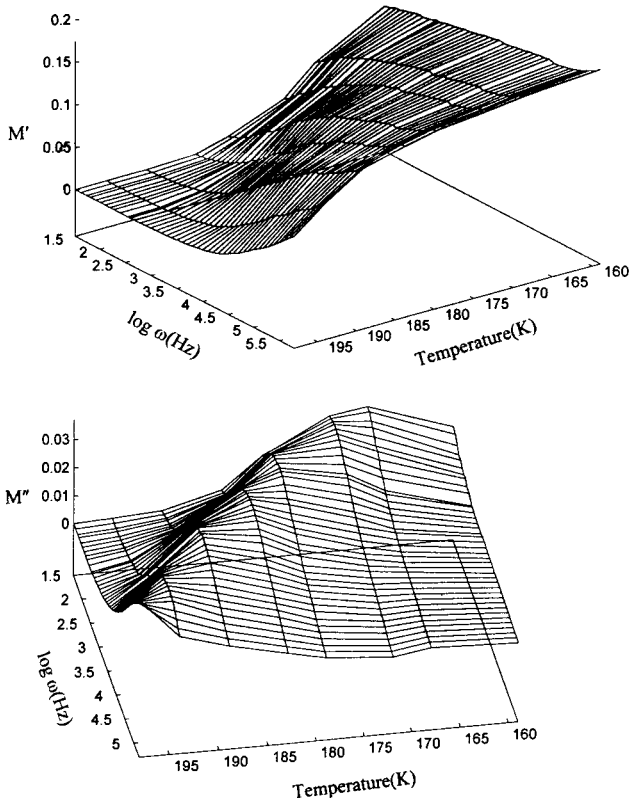

Figure 10. Real (M') and imaginary (M'') component of the electrical modulus of $Cd_{0.75}PS_3Na_{0.5}(H_2O)_2$ as a function of frequency and temperature.

$$M^* = M_\infty\left[1 - \int_0^\infty \exp(-i\omega t)\left(\frac{d\phi(t)}{dt}\right) dt\right] \qquad (3)$$

where $\phi(t)$ is a decay function of the electric field [$E(t) = E(0)\phi(t)$]. M_∞ is the high-frequency limit of the modulus. In the M^* representation, a relaxation peak is observed for the conductivity process in the frequency spectra of the imaginary component of M^*; no peak occurs in the dielectric spectra. Comparisons of the ϵ^* and M^* representations have been used to distinguish localized dielectric relaxation from long-range conductivity.[32]

The real and imaginary components of the modulus spectra of $Cd_{1-x}PS_3Na_{2x}(H_2O)_2$ are shown in Figure 10. The M'' spectrum shows a single well-defined relaxation peak. The corresponding dielectric spectrum, $\epsilon^*(\omega)$, is featureless (Figure 6a−d).

For a quantitative analysis of the modulus data, the decay function, $\phi(t)$, was calculated using the inverse transform of eq 3. Since the real and imaginary components of M^* are connected by the Kramers−Krönig transform, it is sufficient to use only M'' to calculate $\phi(t)$.

$$\phi(t) = \frac{2}{\pi}\int_0^\infty \frac{M''}{M_\infty}\frac{d\omega}{\omega}\cos\omega t \qquad (4)$$

The actual transform was carried out by first fitting the experimental M'' data at each temperature to the imaginary component of the empirical Havriliak−Negami (HN) equation

$$M^*(\omega) = M_\infty\left[1 - \frac{1}{(1 + (i\omega\tau)^\alpha)^\beta}\right] \qquad (5)$$

where $0 \le \alpha, \beta \le 1$ are the shape parameters. The analytical form of eq 5 along with the fitted parameters was transformed

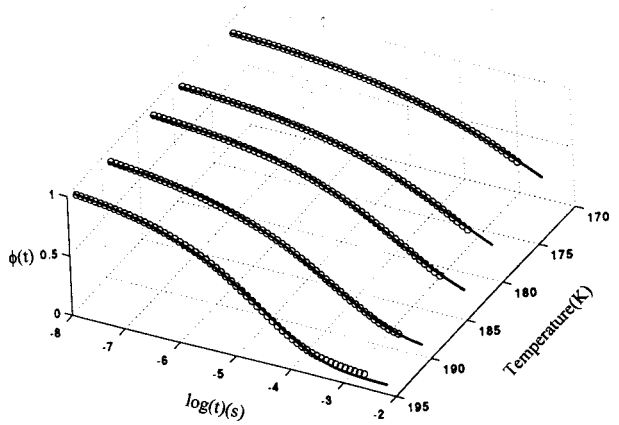

Figure 11. Decay function, $\phi(t)$, for the conductivity relaxation of the double-layer $Cd_{0.75}PS_3Na_{0.5}(H_2O)_2$ at various temperatures. The solid line is the fit to the stretched exponential function (eq 6).

TABLE 2: Temperature Dependence of the Stretched Exponential Fit Parameters Which Describe the Decay Function (Figure 11) Calculated from the Modulus Spectra (Figure 10) of the Double-Layer $Cd_{0.75}PS_3Na_{0.5}(H_2O)_2$

temp (K)	τ_{SE} (s)	β_{SE}	$\langle\tau_\sigma\rangle$ (s)
172	4.75×10^{-3}	0.27	7.67×10^{-2}
179	1.31×10^{-3}	0.29	1.52×10^{-2}
183	3.60×10^{-4}	0.32	2.44×10^{-3}
189	8.96×10^{-5}	0.34	4.87×10^{-4}
194	2.32×10^{-5}	0.40	7.49×10^{-5}

TABLE 3: Comparison of the dc Conductivity Values Calculated from the M'' Spectra with That Obtained from the Complex Admittance

temp (K)	$\sigma_{DC} = \epsilon_0\epsilon_\infty/\langle\tau_\sigma\rangle$ (S/cm)	σ_{DC} (S/cm) (from complex admittance)
172	7.10×10^{-12}	2.00×10^{-11}
179	3.34×10^{-11}	3.46×10^{-11}
183	2.16×10^{-10}	2.34×10^{-10}
189	1.13×10^{-09}	9.35×10^{-10}
194	9.56×10^{-09}	5.14×10^{-09}

using eq 4.[33] The resulting decay functions were found to be asymmetric with respect to time (Figure 11) and are well described by the Kohlrausch−Williams−Watts or stretched exponential decay function

$$\phi(t) = \exp(-t/\tau_{SE})^{\beta_{SE}} \tag{6}$$

with the value of β_{SE} increasing with temperature (Table 2). The departure of β_{SE} from unity characterizes the departure from an ideal Debye relaxation. The average relaxation time associated with the stretched exponential decay function is[30]

$$\langle\tau_\sigma\rangle = \frac{\tau_{SE}}{\beta_{SE}}\Gamma\left(\frac{1}{\beta_{SE}}\right) \tag{7}$$

where Γ is the gamma function. $\langle\tau_\sigma\rangle$ values of $Cd_{1-x}PS_3Na_{2x}(H_2O)_y$, $y = 2$, corresponding to the decay functions of Figure 11 are given in Table 2.

The assignment of the loss feature in the imaginary component of the electrical modulus to a conductivity relaxation may be confirmed by calculating the dc conductivity from the modulus representation,[30] $\sigma_{DC} = \epsilon_0\epsilon_\infty/\langle\tau_\sigma\rangle$. The dc conductivity values so obtained may be compared with the σ_{DC} values obtained from the complex admittance data (Table 3). The agreement is reasonably good, confirming the assignment.

NMR studies had shown that the interlamellar Na ions are mobile and consequently responsible, at least in part, for the dc conductance. There could also be an ionic conductivity contribution due to protons arising from the Bronsted acidity of the hydrated cations similar to that found in the montmorillonites.[6] The fact that only a single modulus peak is observed, for which the calculated conductivity is identical to that from the complex admittance (Table 3), appears to rule out any significant protonic contribution. However a more detailed study of transference numbers is required before ruling out the latter possibility.

The absence of a dielectric loss in $Cd_{1-x}PS_3Na_{2x}(H_2O)_y$, $y = 2$, is rather puzzling. Although the frequency window is limited ($5-10^5$ Hz), the temperature window of the present measurements is fairly wide (30−330 K) (only data up to 170 K are shown in Figure 6). This in conjunction with the fact that the modulus shows a single peak may be interpreted either as (i) the time scale associated with the reorientational motion of the water dipoles is much faster than 10^{-6} s, even at 30 K, or (ii) the reorientational motion and ionic diffusion processes are not separable and consequently show as a single peak in the M'' spectra with no corresponding peak in the ϵ'' spectra. It is not possible from the results of the present investigation to conclude which of these is operative. A detailed study of the temperature-dependent ^{23}Na and ^1H NMR of $Cd_{1-x}PS_3Na_{2x}(H_2O)_y$ is currently in progress to determine whether the motion of the Na ion and water molecules is correlated.

4. Conclusions

Hydrated Na ions have been ion-exchange intercalated into the insulating layered cadmium thiophosphate to give $Cd_{0.75}PS_3Na_{0.5}(H_2O)_y$, $y = 2$. Intercalation occurs with a loss of Cd ions from the $CdPS_3$ layer with electroneutrality being preserved by hydrated Na ions that reside in the interlamellar space. We found that the deintercalation of water occurs via a $Cd_{0.75}PS_3Na_{0.5}(H_2O)_y$ phase with $y = 1$ and lattice expansion 2.8 Å. The conversion of the double-layer $y = 2$ phase to the monolayer $y = 1$ phase is completely reversible (Figure 1). The monolayer phase may be formed from the double-layer phase on evacuation at room temperature and, on exposure adsorbs water from the atmosphere and reverts back to the double-layer, $y = 2$, phase. The negatively charged $Cd_{0.75}PS_3$ layers are electrically inert and consequently the observed electrical response may be attributed, in entirety, to the intercalated guest species. These compounds are, therefore, attractive for studying the influence of the extent of hydration of the guest cation on the electrical behavior.

We have investigated the frequency and temperature dependence of the conductivity and dielectric response in the mono- and double-layer phases of $Cd_{0.75}PS_3Na_{0.5}(H_2O)_y$. The double-layer, $y = 2$, phase is conducting, with a dc conductance of $\sigma_{DC} \sim 10^{-5}$ S/cm at 250 K and an activation energy of 15.8 kcal/mol. The monolayer $y = 1$ phase shows a much poorer conductivity, $\sigma_{DC} \sim 10^{-9}$ S/cm at 250 K. The dielectric permittivity of this compound exhibits a dielectric relaxation at acoustic frequencies which is reasonably well described by the symmetric Cole−Cole distribution, although a fit to the more general Havriliak−Negami distribution had been attempted. This relaxation arises from the reorientation of the dipole moments associated with the water molecule, and the fact that the relaxation times and activation energy are comparable to that for the Debye relaxation in ice suggests that the interlamellar water is fairly rigidly bound, evidently due to the electric field of the cation.

In the conducting $Cd_{0.75}PS_3Na_{0.5}(H_2O)_y$, $y = 2$, phase there is evidence from ^{23}Na NMR that the interlamellar sodium ions are mobile. The dielectric permittivity of this phase is featureless in the $5-10^5$ Hz frequency window down to 30 K. The electrical modulus representation of the same data shows a loss feature in the imaginary component. The relaxation associated with this feature shows a stretched exponential decay. The dc conductivities calculated from the average relaxation time are in good agreement with values obtained from the complex admittance data, and consequently the observed loss in the modulus may be ascribed to a conductivity relaxation. In conclusion, the present study clearly demonstrates the dramatic effect of the extent of hydration of the guest cation on the overall electrical behavior.

Acknowledgment. The authors thank the IISc-ISRO Space Technology Cell for funding. P.J. thanks CSIR (India) for a research fellowship.

References and Notes

(1) Clement, R. *J. Chem. Soc., Chem. Commun.* **1980**, 647.
(2) Clement, R.; Lagadic, I.; Leaustic, A.; Audiere, J. P.; Lomas, L. *Chemical Physics of Intercalation II*; NATO ASI Series, Series B; 1993; p 315.
(3) Brec, R. *Solid State Ionics* **1986**, *22*, 3.
(4) Jeevanandam, P.; Vasudevan, S. *Solid State Ionics* **1997**, *104*, 45.
(5) Poinsignon, S. *Solid State Ionics* **1997**, *97*, 399.
(6) Slade, R. C. T.; Barker, J.; Hirst, P. R.; Halstead, T. K.; Reid, P. I. *Solid State Ionics* **1987**, *24*, 289.
(7) Whittingham, M. S. *Solid State Ionics* **1987**, *25*, 295.
(8) Whittingham, M. S. *Solid State Ionics* **1989**, *32/33*, 344.
(9) Klingen, W.; Ott, R.; Hahn, H. *Z. Anorg. Allg. Chem.* **1973**, *396*, 271.
(10) Ouvrard, G.; Brec, R.; Rouxel, J. *Mater. Res. Bull.* **1985**, *20*, 1181.
(11) Boukamp, B.A. *Solid State Ionics* **1984**, *11*, 339. Jeevanandam, P. Ph.D Thesis, Indian Institute of Science, Bangalore, 1997.
(12) Macedo, P. B.; Moynihan, C. T.; Boese, R. *Phys. Chem. Glasses* **1972**, *13*, 171.
(13) Sposito, G.; Prost, R. *Chem. Rev.* **1982**, *82*, 553.
(14) Jonscher, A. K. *Dielectric Relaxation in Solids*; Chelsea Dielectrics: London, 1983.
(15) Laperche, V.; Lambert, J. F.; Prost, R.; Fripiat, J. J. *J. Phys. Chem.* **1990**, *94*, 8821.
(16) Elliott, S. R. *Adv. Phys.* **1987**, *35*, 135.
(17) Elliott, S. R. *Solid State Ionics* **1988**, *27*, 131.
(18) Maxwell, J. C. *A Treatise on Electricity and Magnetism*; Dover Press: New York, 1954; Vol. I.
(19) Wagner, K. W. *Arch. Elektrotech.* **1914**, *2*, 371.
(20) Dissado, L. A.; Hill, R. M. *J. Chem. Soc., Faraday Trans. 1* **1984**, *80*, 291.
(21) Mehrotra, V.; Giannelis, E. P. *J. Appl. Phys.* **1992**, *72*, 1039.
(22) Jeevanandam, P.; Vasudevan, S. *J. Chem. Phys.* **1998**, *108*, 1206.
(23) Jonscher, A. K. *Philos. Mag.* **1978**, *B38*, 587.
(24) Havriliak, S.; Negami, S. *Polymer* **1967**, *8*, 161.
(25) Böttcher, C. J. F.; Bordewijk, P. *Theory of Electric Polarization*; Elsevier: New York, 1978; Vol. 2.
(26) Hasted, J. B. In *Water a Comprehensive Treatise;* Franks, F., Ed.; Plenum Press: New York, 1975; Vol. 2.
(27) Forslind, E.; Jacobsson, A. In *Water a Comprehensive Treatise;* Franks, F., Ed.; Plenum Press: New York, 1975; Vol. 5, p 247.
(28) Jaccard, C. In *Water and Aqueous Solutions: Structure, Thermodynamics and Transport Processes*; Horne, R. A., Ed.; Wiley Interscience: New York, 1972.
(29) Franks, F. In *Water a Comprehensive Treatise;* Franks, F., Ed.; Plenum Press: New York, 1975; Vol. 1.
(30) Moynihan, C. T.; Boesch, L. P.; Laberge, N. L. *Phys. Chem. Glasses* **1973**, *14*, 122.
(31) Angell, C. A. *Chem. Rev.* **1990**, *90*, 523.
(32) Gerhardt, R. *J. Phys. Chem. Solids* **1994**, *55*, 1491.
(33) Kremer, K.; Boese, D.; Meier, G.; Fischer, E. W. *Prog. Colloid Polym. Sci.* **1989**, *80*, 129.